

**This is a self-archived version of an original article. This version may differ from the original in pagination and typographic details.**

**Author(s):** Even, Julia; Chen, Xiangcheng; Soyly, Arif; Fischer, Paul; Karpov, Alexander; Saiko, Vyacheslav; Saren, Jan; Schlaich, Moritz; Schlathölter, Thomas; Schweikhard, Lutz; Uusitalo, Juha; Wienholtz, Frank

**Title:** The NEXT Project : Towards Production and Investigation of Neutron-Rich Heavy Nuclides

**Year:** 2022

**Version:** Published version

**Copyright:** © 2022 by the authors. Licensee MDPI, Basel, Switzerland.

**Rights:** CC BY 4.0



**Rights url:** <https://creativecommons.org/licenses/by/4.0/>

**Please cite the original version:**

Even, J., Chen, X., Soyly, A., Fischer, P., Karpov, A., Saiko, V., Saren, J., Schlaich, M., Schlathölter, T., Schweikhard, L., Uusitalo, J., & Wienholtz, F. (2022). The NEXT Project : Towards Production and Investigation of Neutron-Rich Heavy Nuclides. *Atoms*, 10(2), Article 59.  
<https://doi.org/10.3390/atoms10020059>

## Article

# The NEXT Project: Towards Production and Investigation of Neutron-Rich Heavy Nuclides

Julia Even <sup>1,\*</sup>, Xiangcheng Chen <sup>1</sup>, Arif Soylu <sup>1</sup>, Paul Fischer <sup>2</sup>, Alexander Karpov <sup>3</sup>, Vyacheslav Saiko <sup>3</sup>, Jan Saren <sup>4</sup>, Moritz Schlaich <sup>5</sup>, Thomas Schlathöler <sup>1</sup>, Lutz Schweikhard <sup>2</sup>, Juha Uusitalo <sup>4</sup> and Frank Wienholtz <sup>5</sup>

<sup>1</sup> Faculty of Science and Engineering, University of Groningen, 9701 BA Groningen, The Netherlands; xiangcheng.chen@rug.nl (X.C.); a.soylu@rug.nl (A.S.); t.a.schlatholter@rug.nl (T.S.)

<sup>2</sup> Institut für Physik, Universität Greifswald, 17487 Greifswald, Germany; paul.fischer@uni-greifswald.de (P.F.); lschweik@physik.uni-greifswald.de (L.S.)

<sup>3</sup> Joint Institute for Nuclear Research, 141980 Dubna, Russia; karpov@jinr.ru (A.K.); saiko@jinr.ru (V.S.)

<sup>4</sup> Department of Physics, University of Jyväskylä, 40014 Jyväskylä, Finland; jan.saren@jyu.fi (J.S.); juha.uusitalo@jyu.fi (J.U.)

<sup>5</sup> Institut für Kernphysik, Technical University of Darmstadt, 64289 Darmstadt, Germany; mschlaich@ikp.tu-darmstadt.de (M.S.); fwienholtz@ikp.tu-darmstadt.de (F.W.)

\* Correspondence: j.even@rug.nl; Tel.: +31-50-363-3618

**Abstract:** The heaviest actinide elements are only accessible in accelerator-based experiments on a one-atom-at-a-time level. Usually, fusion–evaporation reactions are applied to reach these elements. However, access to the neutron-rich isotopes is limited. An alternative reaction mechanism to fusion–evaporation is multinucleon transfer, which features higher cross-sections. The main drawback of this technique is the wide angular distribution of the transfer products, which makes it challenging to catch and prepare them for precision measurements. To overcome this obstacle, we are building the NEXT experiment: a solenoid magnet is used to separate the different transfer products and to focus those of interest into a gas-catcher, where they are slowed down. From the gas-catcher, the ions are transferred and bunched by a stacked-ring ion guide into a multi-reflection time-of-flight mass spectrometer (MR-ToF MS). The MR-ToF MS provides isobaric separation and allows for precision mass measurements. In this article, we will give an overview of the NEXT experiment and its perspectives for future actinide research.

**Keywords:** NEXT; neutron-rich nuclei; multinucleon transfer; solenoid separator; mass spectrometer



**Citation:** Even, J.; Chen, X.; Soylu, A.; Fischer, P.; Karpov, A.; Saiko, V.; Saren, J.; Schlaich, M.; Schlathöler, T.; Schweikhard, L.; et al. The NEXT Project: Towards Production and Investigation of Neutron-Rich Heavy Nuclides. *Atoms* **2022**, *10*, 59.

<https://doi.org/10.3390/atoms10020059>

Academic Editors: Mustapha Laatiaoui and Sebastian Raeder

Received: 28 March 2022

Accepted: 26 May 2022

Published: 1 June 2022

**Publisher's Note:** MDPI stays neutral with regard to jurisdictional claims in published maps and institutional affiliations.



**Copyright:** © 2022 by the authors. Licensee MDPI, Basel, Switzerland. This article is an open access article distributed under the terms and conditions of the Creative Commons Attribution (CC BY) license (<https://creativecommons.org/licenses/by/4.0/>).

## 1. Introduction

Access to the heaviest elements in the periodic table is limited. While elements up to einsteinium and fermium are still available in macro-amounts, all heavier elements are only accessible in accelerator-based experiments on a one-atom-at-a-time scale. Workhorses for the production of the transfermium elements are fusion–evaporation reactions [1], which are restricted by the availability of target materials and ion beams, as well as by the reaction cross-sections. An alternative reaction mechanism that can be applied and that gives access to isotopes further on the neutron-rich side are deep inelastic collisions resulting in multinucleon transfer [2–6]. Multinucleon transfer reactions have been known for decades as a means for accessing neutron-rich transfermium isotopes. However, their application in studying transfermium isotopes is still limited.

Similar to experiments using fusion reactions, an intense ion beam (of typically 0.5 particle nA up to 2 particle  $\mu$ A) impinges on a target foil with a thickness of a few microns. The various products of the fusion–evaporation reactions continue flying in beam direction and can be separated by an electromagnetic separator. In deep inelastic collisions, a neck is formed between the projectile and the target nucleus. Nucleons are exchanged; the system rotates and splits again. The reaction products are emitted in a large polar angle of 30° to 60°

with respect to the beam axis, which limits the collection of multinucleon transfer products for subsequent precision studies. Electromagnetic separators such as SHIP [2], VAMOS [7], or PRISMA [8] cannot cover the whole solid angle and are only able to capture a fraction of the products. Studies of transfer products using radiochemical separation techniques are limited to long-lived isotopes [4]. In recent years, new experiments, in which gas-cells are directly placed behind the target to stop and capture a large fraction of the transfer products, have been developed, such as the KISS experiment [9], the  $N = 126$  factory [10], and experiments at IGISOL [11] and at the FRS gas-catcher [12]. All these experiments require an additional separation step. In the case of the KISS experiment, laser ionization of the products is applied.

Here, we report about a new setup called NEXT that is currently being built at the AGOR cyclotron in Groningen. The NEXT setup shall fulfill the following requirements:

- a large angular acceptance to capture the vast majority of the target-like transfer products and achieve good focusing;
- good suppression of the primary beam and lighter transfer products;
- separation and identification of isobaric nuclides;
- isotope identification independent from chemical properties
- sensitivity to isotopes of a broad range of half-lives.

To achieve this demand, the heavy target-like transfer products are pre-separated by their magnetic rigidity from the primary beam and the light projectile-like products within a superconducting solenoid magnet [13]. The target-like products are focused towards the end of the solenoid, where they are stopped in a gas-catcher [14]. The transfer products are extracted and bunched by a stacked-ring ion guide [15] before they are injected into a multi-reflection time-of-flight mass spectrometer (MR-ToF MS) [16–18] for isobaric separation and mass measurements. Figure 1 shows a schematic overview of the setup.

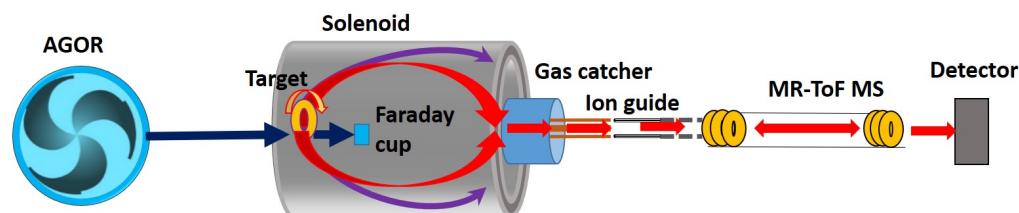


**Figure 1.** Schematic overview of the NEXT setup. The dark arrows indicate the primary beam. The red arrows indicate the trajectories of target-like fragments, while the purple arrows indicate the trajectories of the projectile-like fragments.

## 2. The NEXT Setup

### 2.1. AGOR Cyclotron

The primary intense ion beam is delivered by the AGOR cyclotron in Groningen [19]. AGOR is a superconducting cyclotron with a cyclotron K value (bending limit) of 600 MeV that is capable of accelerating light and heavy ions in a range of energies, from 5 MeV/u for heavy ions and up to 190 MeV for protons, as practically continuous beams. It is equipped with an electron cyclotron resonance (ECR) ion source, which provides a broad range of stable beams up to lead. Beam intensities depend on the desired projectiles and range from an particle nA to a few particle  $\mu\text{A}$  [20]. Based on the experience with various projectiles and ion-source tests, we expect beam currents at the target position of the NEXT experiment in the order of hundreds of particles nA .

### 2.2. The Solenoid Separator

The primary beam from AGOR is focused on the target, which is located inside a solenoid magnet. The un-reacted beam is collected by a Faraday cup behind the target. The target can be moved along the central axis of the magnet. The magnet had previously been part of a magnetic resonance imaging apparatus. Its total length is 160 cm, and the inner diameter is about 90 cm. It provides a magnetic flux density of  $B = 3$  T. The trajectories

of the transfer-product ions recoiling out from the target are bent depending on the emitting angle and the magnetic rigidity  $B\rho = \frac{p}{q}$  of the ions, where  $\rho$  is the gyroradius of the ion due to the magnetic field,  $p$  is its momentum, and  $q$  is its charge state.

In order to optimize the transmission of target-like products towards the gas-catcher and their separation from projectile-like fragments, two model reactions were chosen:

- $^{136}\text{Xe} + ^{198}\text{Pt}$  at an energy of 6 MeV/u to produce nuclei around  $N = 126$  [21];
- $^{48}\text{Ca} + ^{251}\text{Cf}$  at an energy of 6.1 MeV/u to produce transfermium nuclei [22].

To simulate the trajectories of the reaction products, the differential cross-section, the emitting angle from the target, the kinetic energy, and the charge-states of the ions of interest are required as input data. The differential cross-section of the various isotopes, the emitting angle, and the kinetic energies of the ions are taken from predictions made by a dynamical model based on the Langevin equations [21,22]. This model provides a continuous description of the time evolution of the system of colliding nuclei, starting from the approaching stage of the projectile and the target in the entrance channel of the reaction, and up to the formation of the final reaction products. The stochastic nature of the interaction between two colliding nuclei is taken into account in this model. This leads to the formation of products in a wide range of masses, energies, and scattering angles. The model gives a reasonable description of various characteristics of the products of multinucleon transfer reactions that was verified on a large set of available experimental data. The mean charge states of the ions were calculated using an empirical charge state formula for heavy ions, according to reference [23]. The distributions of the charge states were calculated according to reference [24]. Figure 2 shows two examples of the resulting acceptance region of the solenoid separator. The green areas indicate the emitting angle and magnetic rigidity of ions that will be transmitted from a target towards the gas-catcher. Ions emitted in a small angle are stopped by a cylindrical Faraday cup of 6.2 cm radius and 12.4 cm length, which is placed a few centimeters behind the target. By changing the target position, the acceptance region can be adjusted. As an example for neutron-rich transfermium nuclei  $^{261}\text{Md}$  produced in the reaction  $^{48}\text{Ca} + ^{251}\text{Cf}$  at an energy of 6.1 MeV/u was chosen. The magnetic rigidity and angular distribution of  $^{261}\text{Md}$  ( $Z = 101$ ) is indicated by the solid lines in Figure 2A. They overlap, to a large degree, with the acceptance region of the magnet. The transmission efficiencies of the target-like products of the model reaction  $^{48}\text{Ca} + ^{251}\text{Cf}$  are summarized in Figure 3. The figure shows the suppression of recoiling nuclei that are close to the nuclear mass and charge of the target material. The transfer products, which are heavier than the target material, are emitted within the acceptance region of the solenoid and, therefore, high-transmission yields around 80% can be achieved.

In order to optimize for  $N = 126$  nuclei, the transmission of the products of the reaction  $^{136}\text{Xe} + ^{198}\text{Pt}$  at an energy of 6 MeV/u was investigated. The magnetic rigidity of  $N = 126$  nuclei is higher than the rigidity of the transfermium isotopes produced in  $^{48}\text{Ca} + ^{251}\text{Cf}$ , and, thus, they lie only partially within the acceptance region of the magnet (see Figure 2B). The optimum target position for the reaction  $^{136}\text{Xe} + ^{198}\text{Pt}$  was determined to be 70 cm inside the solenoid, and typical transmission yields of about 15% could be reached. The projectile-like fragments lie, to a large degree, outside the acceptance region; thus, they are efficiently suppressed by the solenoid separator.

### 2.3. Gas-Catcher, Ion Guide, and MR-ToF MS

The transmitted target-like transfer products pass the titanium entrance window of the gas-catcher [14] placed behind the solenoid. The ions are slowed down by collisions with the gas atoms inside the gas catcher, which has a length of 45 cm and a diameter of 40 cm. The ions are guided by a direct current (DC) gradient towards the backside of a gas-catcher, where a radiofrequency (RF) carpet is located. The RF carpet is a printed circuit board with concentric ring electrodes and an electrode gap of 0.125 mm. The ions are transported by a DC gradient of 3 V/cm and an RF potential of 80 V peak-to-peak and at a frequency of 5.7 MHz towards the center, from where they are extracted through a hole of 0.45 mm diameter by a supersonic gas flow. The ions are, thus, emitted from the gas-catcher as a continuous, divergent beam with energies of a few electron volts. In order

to inject the ions into the MR-ToF MS, the beam needs to be transformed into well-focused ion bunches with energies of a few kiloelectron volts. To this end, an ion guide consisting of a stack of rings has been developed.

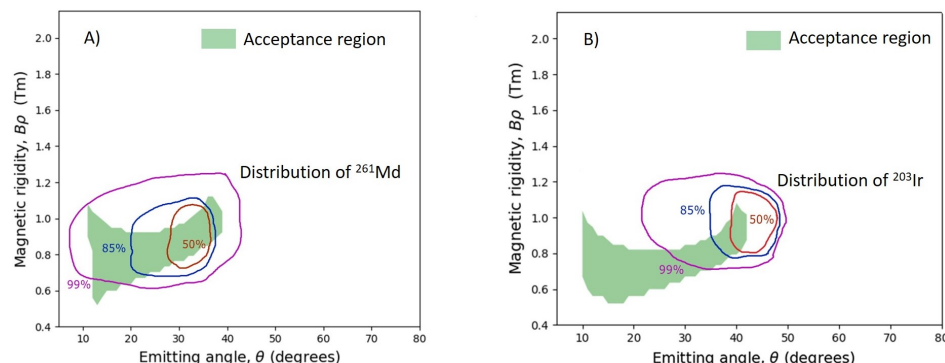


**Figure 2.** Acceptance plots of the solenoid separator. The green areas indicate the acceptance region of the solenoid magnet. Ions with corresponding magnetic rigidities and emitting angles that are released from a target placed behind the solenoid will reach the entrance window of the gas-catcher. (A) shows the acceptance region when the target is placed 53 cm inside the magnet. The distance between the target and the Faraday cup is 32 cm, and the distance between the gas-catcher and the end of the solenoid is 70 cm. The solid lines represent the distribution of  $^{261}\text{Md}$  ions produced in the reaction  $^{48}\text{Ca} + ^{251}\text{Cf}$  at an energy of 6.1 MeV/u. (B) shows the acceptance region when the target is placed 69 cm inside the magnet. The distance between the target and the Faraday cup is 32 cm, and the distance between the gas-catcher and the end of the solenoid is 72 cm. The solid lines represent the distribution of  $^{203}\text{Ir}$  ions produced in the reaction  $^{136}\text{Xe} + ^{198}\text{Pt}$  at an energy of 6.0 MeV/u.

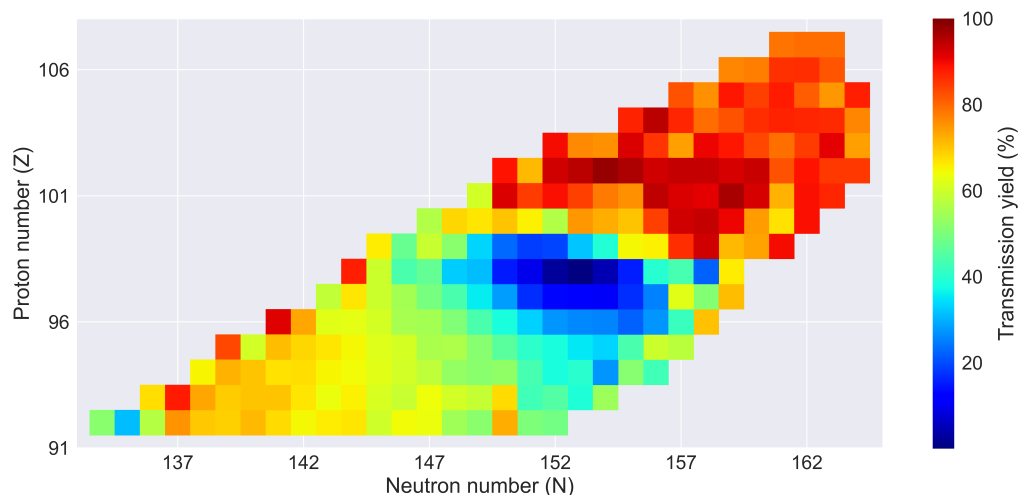


**Figure 3.** Transmission yields of nuclides produced in the reaction  $^{48}\text{Ca} + ^{251}\text{Cf}$  at an energy of 6.1 MeV/u.

Figure 4 shows the model of the novel stacked-ring ion guide. Details concerning its design and the simulation of the ion transmission efficiency can be found in reference [15]. The ion guide consists of a stack of 78 ring electrodes. The ions are confined radially by an RF potential. To capture the divergent beam from the gas-catcher, the first ring has the widest inner diameter (14 mm). The inner diameters over the first eight rings decrease in order to focus the ions. Behind the focusing section of the ion guide, the thermalization section follows (see Figure 4), which consists of 60 identical rings. Here, the ions reach thermal equilibrium by interaction with the buffer gas and are transported by a travelling wave of bias voltages. From the thermalization section, the ions enter the refocusing section consisting of five rings with decreasing inner diameters. From there, the ions reach the bunching section, which consists of five rings. Here, the ions are accumulated until they



are ejected as an ion bunch by disconnecting the last four rings from the RF voltage and applying optimized ejecting voltages. According to our simulations, the transmission efficiency of the ion guide is 80%. The energy and time spreads of ion bunches at the one-sigma level are 3.66 eV and 0.06  $\mu\text{s}$ , respectively.

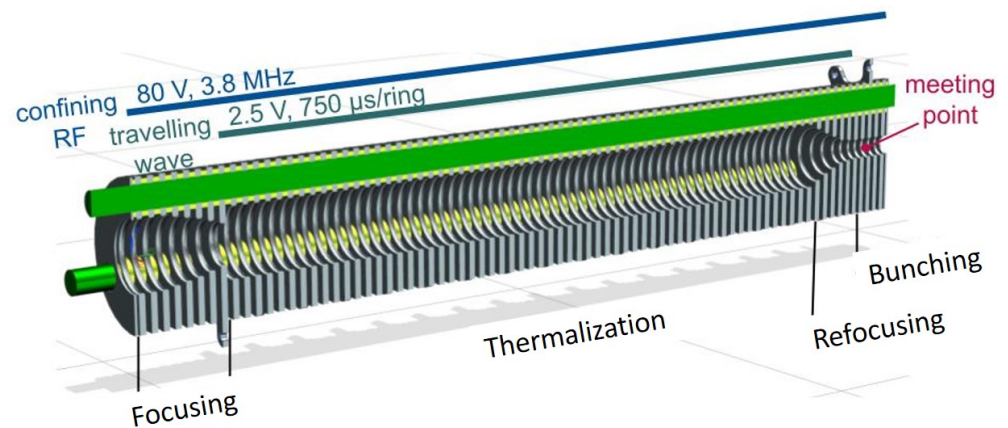


**Figure 4.** Design of the stacked-ring ion guide. The ions leaving the gas-catcher are captured in the focusing section. They are transported by a travelling wave towards the refocusing and the bunching section, from where they are ejected.

Figure 5 shows the model of the gas-catcher, the ion-guide section, and the MR-ToF MS. The gas-catcher is operated at a pressure of 50 mbar. The gas streaming through the exit hole of the gas-catcher is pumped away by a turbo-molecular pump with a pump capacity of 2200 L/s (pump 1, Figure 5), resulting in a pressure of about  $10^{-3}$  mbar at the ring ion guide section. The operation of the MR-ToF MS requires a vacuum in the order of  $10^{-9}$  mbar. Therefore, differential pumping is implemented. The ion guide section is separated by a 2 mm wide pulsed drift tube from a set of ion lenses. In this section, a turbo molecular pump with a capacity of 350 L/s (pump 2) is installed, and a pressure of  $10^{-7}$  mbar is reached. This section is separated by an iris from the section of the MR-ToF analyzer, where another pump with a capacity of 700 L/s (pump 3) is installed in order to reach  $10^{-9}$  mbar.

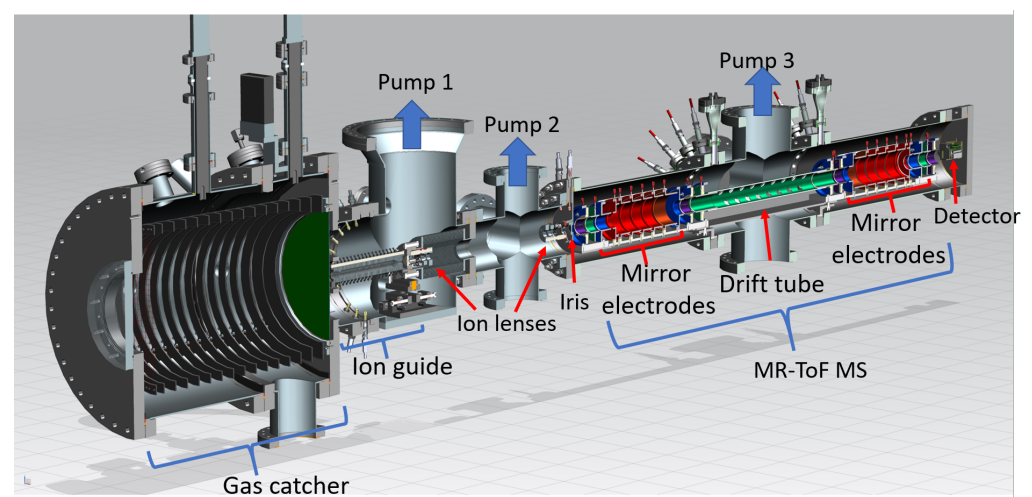


**Figure 5.** Drawing of the gas-catcher coupled by the ion guide to the MR-ToF MS.

The ion bunches ejected from the ring ion guide are refocused by the set of lenses; they pass the iris and are injected into the MR-ToF MS.

The MR-ToF MS has been developed at the Technical University of Darmstadt [16] and is currently under construction. It consists of two electrostatic ion-optical mirrors which are

connected by a 70 cm long drift tube with a pulsable potential. For the injection and ejection of the ions, the “in-trap potential lift method” will be used [25]: the ions are injected into the MR-ToF MS, while the drift tube is on high potential. When the ions are inside, the potential of the drift tube is lowered and the ions are trapped between the mirrors and are reflected multiple times. By increasing the potential of the drift tube, the ions are ejected in mass-separated bunches and sent to a multichannel plate (MCP) detector to determine the time of flight. The MR-ToF method allows for mass measurements with a resolving power of several hundred thousands [17,18], as well as for isobaric separation to prepare purified samples for decay spectroscopy. Due to their different velocities, the ions of interest can be separated even from isobaric species, either during the storage period [26] or by the timing and duration of the ejection pulse [27]. For the spectroscopy, the MCP detector will be replaced by a silicon detector that is sensitive to alpha particles and fission fragments. The detection station is designed in such a way that it can be easily upgraded and the detectors can be exchanged.

### 3. Status and Planned Experimental Program

Currently, the NEXT experiment is in the late design phase. The machining and installation of several parts has already started. The ion guide and MR-ToF components are under construction, and the solenoid magnet will arrive at AGOR in Summer 2022.

NEXT will open the door to nuclei around the third waiting point for the r-process of nucleosynthesis at the neutron shell closure around  $N = 126$  [28]. These nuclei will be accessed through  $^{136}\text{Xe}$ -induced reactions, and their mass will be determined by the MR-ToF MS. The expected rates of  $^{203}\text{Ir}$  and neighboring isotopes and isotones lie in the order of a few hundred ions per second at the focal point of the solenoid. The first mass-measurement campaigns at NEXT will focus on this region of the nuclear chart. Furthermore, NEXT will study neutron-rich nuclei in the transfermium region. These will be accessible through asymmetric reactions with actinide targets. The focus of the first experiments will lie in the mendelevium region towards the neutron subshell closure at  $N = 162$ , where we expect rates of a few ions per minute at the focal plane of the solenoid. For the simulations, we focused on the medium-mass projectile  $^{48}\text{Ca}$ . However, as day-one experiments, we plan to also use beams that are easier to develop, such as  $^{18}\text{O}$  and  $^{22}\text{Ne}$ . After commissioning, we plan to focus on the masses and fission half-lives of the neutron-rich isotopes in the transfermium region.

### 4. Conclusions

NEXT will provide a new step to the neutron-rich side of the chart of nuclei. It will give access to isotopes that are difficult to reach at other facilities. The solenoid separator will allow for the separation of target-like transfer products from the primary beam and projectile-like fragments. The coupling to the MR-ToF MS through a gas-catcher and stacked-ring ion guide will prepare samples for decay studies and will allow the mass measurements of very exotic isotopes with high precision.

**Author Contributions:** Conceptualization, J.E.; simulation and design of the solenoid separator, A.S., J.S., J.U., and J.E.; theoretical predictions of the nuclear reactions/nuclear input data for the simulations, A.K. and V.S.; simulation and design of the ion guide, X.C., J.E., and T.S.; design and development of the MR ToF MS, M.S., F.W., L.S., and P.F.; writing—original draft preparation, J.E.; writing—review and editing, all authors; visualization, A.S., X.C., and J.E.; supervision, J.E.; project administration, J.E.; funding acquisition, J.E. All authors have read and agreed to the published version of the manuscript.

**Funding:** This research was funded by the European Research Council Executive Agency (ERCEA), under the powers delegated by the European Commission through a starting grant number 803740—NEXT—ERC-2018-STG.

**Institutional Review Board Statement:** Not applicable.

**Informed Consent Statement:** Not applicable.

**Data Availability Statement:** Data of the simulation are available upon request.

**Acknowledgments:** We would like to thank Nathanael Moorrees and Henk Smit for their technical support and help with the drawings. Furthermore, we would like to thank the workshops at the PARTREC facility at UMCG, Groningen, for their support.

**Conflicts of Interest:** The authors declare no conflict of interest.

### Abbreviations

The following abbreviations are used in this manuscript:

NEXT	Neutron-rich, EXotic, heavy nuclei produced in multi-nucleon Transfer reactions
MR-ToF MS	Multi-reflection time-of-flight mass spectrometer
SHIP	Separator for heavy ion reaction products
VAMOS	Variable mode spectrometer
KISS	KEK isotope separation system
IGISOL	Ion guide isotope separation on-line
FRS	Fragment separator
AGOR	Accélérateur Groningen–Orsay
ECR	Electron cyclotron resonance
N	Neutron number
DC	Direct current
RF	Radiofrequency
MCP	Multichannel plate

### References

1. Türler, A.; Pershina, V. Advances in the production and chemistry of the heaviest elements. *Chem. Rev.* **2013**, *113*, 1237–1312. <https://doi.org/10.1021/cr3002438>.
2. Devaraja, H.M.; Heinz, S.; Ackermann, D.; Göbel, T.; Heßberger, F.P.; Hofmann, S.; Maurer, J.; Münzenberg, G.; Popeko, A.G.; Yeremin, A.V. New studies and a short review of heavy neutron-rich transfer products. *Eur. Phys. J. A* **2020**, *56*, 1–17. <https://doi.org/10.1140/epja/s10050-020-00229-2>.
3. Loveland, W.D. The Synthesis of New Neutron-Rich Heavy Nuclei. *Front. Phys.* **2019**, *7*, 1–8. <https://doi.org/10.3389/fphy.2019.00023>.
4. Kratz, J.V.; Loveland, W.; Moody, K.J. Syntheses of transuranium isotopes with atomic numbers  $Z \leq 103$  in multi-nucleon transfer reactions. *Nucl. Phys. A* **2014**, *944*, 117–157. <https://doi.org/10.1016/j.nuclphysa.2015.06.004>.
5. Zagrebaev, V.I.; Greiner, W. Cross sections for the production of superheavy nuclei. *Nucl. Phys. A* **2014**, *944*, 257–307. <https://doi.org/10.1016/j.nuclphysa.2015.02.010>.
6. Corradi, L.; Szilner, S.; Pollarolo, G.; Montanari, D.; Fioretto, E.; Stefanini, A.M.; Valiente-Dobón, J.J.; Farnea, E.; Michelagnoli, C.; Montagnoli, G.; et al. Multinucleon transfer reactions: Present status and perspectives. *Nucl. Instrum. Methods Phys. Res. Sect. B Beam Interact. Mater. Atoms* **2013**, *317*, 743–751. <https://doi.org/10.1016/j.nimb.2013.04.093>.
7. Golabek, C.; Heinz, S.; Mittig, W.; Rejmund, F.; Villari, A.C.C.; Bhattacharyya, S.; Boilley, D.; de France, G.; Drouart, A.; Gaudefroy, L.; et al. Investigation of deep inelastic reactions in  $^{238}\text{U} + ^{238}\text{U}$  at Coulomb barrier energies. *Eur. Phys. J. A* **2010**, *43*, 251–259. <https://doi.org/10.1140/epja/i2010-10911-5>.
8. Vogt, A.; Birkenbach, B.; Reiter, P.; Corradi, L.; Mijatovic, T.; Montanari, D.; Szilner, S.; Bazzacco, D.; Bowry, M.; Bracco, A.; et al. Light and heavy transfer products in  $\text{Xe-136} + \text{U-238}$  multinucleon transfer reactions. *Phys. Rev. C Nucl. Phys.* **2015**, *92*, 1–12. <https://doi.org/10.1103/PhysRevC.92.024619>.
9. Watanabe, Y.; Hirayama, Y.; Imai, N.; Ishiyama, H.; Jeong, S.; Miyatake, H.; Clement, E.; de France, G.; Navin, A.; Rejmund, M.; et al. Study of collisions of  $\text{Xe-136} + \text{Pt-198}$  for the KEK isotope separator. *Nucl. Instrum. Methods Phys. Res. Sect. B Beam Interact. Mater. Atoms* **2013**, *317*, 752–755. <https://doi.org/10.1016/j.nimb.2013.04.036>.
10. Savard, G.; Brodeur, M.; Clark, J.A.; Knaack, R.A.; Valverde, A.A. The  $N = 126$  factory: A new facility to produce very heavy neutron-rich isotopes. *Nucl. Instrum. Methods Phys. Res. Sect. B Beam Interact. Mater. Atoms* **2020**, *463*, 258–261. <https://doi.org/10.1016/j.nimb.2019.05.024>.
11. Spătaru, A.; Balabanski, D.L.; Beliuskina, O.; Constantin, P.; Dickel, T.; Hornung, C.; Kankainen, A.; Karpov, A.V.; Nichita, D.; Plass, W.; et al. Production of exotic nuclei via MNT reactions using gas cells. *Acta Phys. Pol. B* **2020**, *51*, 817–822. <https://doi.org/10.5506/APhysPolB.51.817>.
12. Dickel, T.; Kankainen, A.; Spătaru, A.; Amanbayev, D.; Beliuskina, O.; Beck, S.; Constantin, P.; Benyamin, D.; Geissel, H.; Gröf, L.; et al. Multi-nucleon transfer reactions at ion catcher facilities—A new way to produce and study heavy neutron-rich nuclei. *J. Phys. Conf. Ser.* **2020**, *1668*. <https://doi.org/10.1088/1742-6596/1668/1/012012>.
13. Dvorak, J.; Block, M.; Düllmann, C.; Heinz, S.; Herzberg, R.D.; Schädel, M. IRIS—Exploring new frontiers in neutron-rich isotopes of the heaviest elements with a new Inelastic Reaction Isotope Separator. *Nucl. Instrum. Methods Phys. Res. Sect. A Accel. Spectrometers Detect. Assoc. Equip.* **2011**, *652*, 687–691. <https://doi.org/10.1016/j.nima.2010.08.124>.



14. Mollaebrahimi, A.; Anđelić, B.; Even, J.; Block, M.; Eibach, M.; Giacoppo, F.; Kalantar-Nayestanaki, N.; Kaleja, O.; Kremers, H.R.; Laatiaoui, M.; et al. A setup to develop novel Chemical Isobaric SEparation (CISE). *Nucl. Instrum. Methods Phys. Res. Sect. B Beam Interact. Mater. Atoms* **2020**, *463*, 508–511. <https://doi.org/10.1016/j.nimb.2019.03.018>.
15. Chen, X.; Even, J.; Fischer, P.; Schlaich, M.; Schlathölter, T.; Schweikhard, L.; Soylu, A. Stacked-ring ion guide for cooling and bunching rare isotopes. *Int. J. Mass Spectrom.* **2022**, *477*, 116856. <https://doi.org/10.1016/j.ijms.2022.116856>.
16. Schlaich, M. Development and Characterization of a Multi-Reflection Time-of-Flight Mass Spectrometer for the Offline Ion Source of PUMA. Master's Thesis, Technische Universität Darmstadt, Darmstadt, Germany, 2021.
17. Wolf, R.N.; Wienholtz, F.; Atanasov, D.; Beck, D.; Blaum, K.; Borgmann, C.; Herfurth, F.; Kowalska, M.; Kreim, S.; Litvinov, Y.A.; et al. ISOLTRAP's multi-reflection time-of-flight mass separator/spectrometer. *Int. J. Mass Spectrom.* **2013**, *349–350*, 123–133. <https://doi.org/10.1016/j.ijms.2013.03.020>.
18. Wienholtz, F.; Beck, D.; Blaum, K.; Borgmann, C.; Breitenfeldt, M.; Cakirli, R.B.; George, S.; Herfurth, F.; Holt, J.D.; Kowalska, M.; et al. Masses of exotic calcium isotopes pin down nuclear forces. *Nature* **2013**, *498*, 346–349. <https://doi.org/10.1038/nature12226>.
19. Brandenburg, S.; Ostendorf, R.; Hofstee, M.; Kiewiet, H.; Beijers, H. The irradiation facility at the AGOR cyclotron. *Nucl. Instrum. Methods Phys. Res. Sect. B Beam Interact. Mater. Atoms* **2007**, *261*, 82–85. <https://doi.org/10.1016/j.nimb.2007.04.304>.
20. Brandenburg, S.; Hevinga, M.A.; Nijboer, T.W.; Vorenholt, H. Beam loss monitoring and control for high intensity beams at the AGOR-facility. In Proceedings of CYCLOTRONS 2010, Lanzhou, China, 6–10 September 2010; pp. 227–229.
21. Karpov, A.; Saiko, V. Production of neutron-rich nuclides in the vicinity of  $N = 126$  shell closure in multinucleon transfer reactions. *EPJ Web Conf.* **2017**, *163*, 27. <https://doi.org/10.1051/epjconf/201716300027>.
22. Karpov, A.; Saiko, V. Synthesis of Transuranium Nuclei in Multinucleon Transfer Reactions at Near-Barrier Energies. *Phys. Part. Nucl. Lett.* **2019**, *16*, 667–670. <https://doi.org/10.1134/S1547477119060475>.
23. Shima, K.; Ishihara, T.; Mikumo, T. Empirical formula for the average equilibrium charge-state of heavy ions behind various foils. *Nucl. Instrum. Methods Phys. Res.* **1982**, *200*, 605–608. [https://doi.org/10.1016/0167-5087\(82\)90493-8](https://doi.org/10.1016/0167-5087(82)90493-8).
24. Nikolaev, V.; Dmitriev, I. On the equilibrium charge distribution in heavy element ion beams. *Phys. Lett. A* **1968**, *28*, 277–278. [https://doi.org/10.1016/0375-9601\(68\)90282-X](https://doi.org/10.1016/0375-9601(68)90282-X).
25. Wolf, R.N.; Marx, G.; Rosenbusch, M.; Schweikhard, L. Static-mirror ion capture and time focusing for electrostatic ion-beam traps and multi-reflection time-of-flight mass analyzers by use of an in-trap potential lift. *Int. J. Mass Spectrom.* **2012**, *313*, 8–14. <https://doi.org/10.1016/j.ijms.2011.12.006>.
26. Fischer, P.; Knauer, S.; Marx, G.; Schweikhard, L. In-depth study of in-trap high-resolution mass separation by transversal ion ejection from a multi-reflection time-of-flight device. *Rev. Sci. Instrum.* **2018**, *89*, 015114. <https://doi.org/10.1063/1.5009167>.
27. Wienholtz, F.; Kreim, S.; Rosenbusch, M.; Schweikhard, L.; Wolf, R.N. Mass-selective ion ejection from multi-reflection time-of-flight devices via a pulsed in-trap lift. *Int. J. Mass Spectrom.* **2017**, *421*, 285–293. <https://doi.org/10.1016/j.ijms.2017.07.016>.
28. Cowan, J.J.; Sneden, C.; Lawler, J.E.; Aprahamian, A.; Wiescher, M.; Langanke, K.; Martinez-Pinedo, G.; Thielemann, F.K. Origin of the heaviest elements: The rapid neutron-capture process. *Rev. Mod. Phys.* **2021**, *93*, 15002. <https://doi.org/10.1103/RevModPhys.93.015002>.